Reply to comments of RC2:

This manuscript presents EMAC simulations of global aerosol mass, composition and number from the surface to 10 hPa using a new GMXe modal configuration ("TropStrat", TS) that unifies previously separate tropospheric and stratospheric setups, evaluated against an unusually broad observational suite and then used to describe global aerosol distributions across four atmospheric layers.

I regard this as a valuable contribution, for three reasons. First, the experimental design is clean: running all three modal configurations under QCTM conditions with ERA5 and QBO nudging isolates the effect of the size distribution from chemistry–dynamics feedback, and Fig. 7 demonstrates this convincingly. Second, the observational sampling protocol in Sect. 2.3 is exemplary; converting vacuum aerodynamic to volume-equivalent diameter, integrating the modal PSD over each instrument's size cut, and applying the HR-AMS transmission curve explicitly removes a class of error that has confused earlier comparisons in this domain. Third, the diagnosis of the stratospheric dust problem, which related to emit 900 nm dust into a mode with median diameter near 200 nm effectively down-scales the particle, suppressing sedimentation and enhancing convective lofting.

We thank the referee for the time to review our manuscript, the positive assessment of our manuscript, and the constructive feedback. We report the comments (grey, bold) along with our replies (blue). Text changes are provided in red.

My concerns are not with the direction of the results but with the strength of the quantitative claims relative to the documentation provided. The most consequential methodological change, the dust and sea salt emission size mapping, is described in one sentence with no numbers; the TS setup differs from its predecessors in several respects that are not separated; the term "primary particles," on which the abstract's most novel claim rests, is never defined; and the headline percentages carry no uncertainty. None of this calls the results themselves into question, and all of it can be resolved through documentation, clearer definitions, and more carefully bounded language rather than new simulations.

We acknowledge the constructive criticism on the documentation of the methodology, and improve the manuscript according to the referee's suggestions (see below).

Main comments

1. The species-to-mode emission mapping is not documented anywhere in the manuscript

The manuscript never states which species are emitted into which modes. Section 2.2 says only that "Sea salt and dust emission size distributions were adjusted to the new modal size distributions" (l. 198–199); Sect. 2.2.1 adds that "a substantial amount emitted directly into the small coarse mode" (l. 253); for the previous

setups we learn only that dust was "partly emitted into the accumulation mode" (l. 597). The mode descriptions at l. 231–237 are qualitative. Nowhere is there a figure or table giving the emission mapping.

This is the paper's central methodological change, and the Conclusions attribute its most novel finding directly to it (l. 645). As current description, a reader cannot reproduce or assess it. I would ask for a single table for each mode in two setups:

- (a) which primary species are emitted directly into it (desert dust, sea salt, BC, POA, anthropogenic and biomass-burning primaries, aircraft emissions), and the fraction of each species' emitted mass and number so assigned;
- (b) whether each species enters the soluble mode, the insoluble mode, or both, and in what proportion;

Relatedly, the claim that dust and sea salt emissions "typically peak between 800 and 1000 nm" (l. 252–253) carries no citation and is the physical justification for where the new mode was placed; please clarify whether this refers to a number- or mass-weighted peak and provide a supporting reference.

We agree with the referee that more detail on the species-to-mode emission mapping and the general modal configuration is very helpful for the reader and increases the transparency of the methodology. We additionally provide three new tables (one in the main text, and two in the supplement)

First, we provide an additional main text table summarizing, which species are treated in which modes, and how species (mass) can enter these modes (Table 1 here).

Table 1: (Table 2 of the revised manuscript) Species to mode mapping with the relevant processes for mass and number accumulation in the respective modes: primary emission; nucleation; growth- or evaporation-driven transfer from neighbouring modes; inter-modal coagulation; ageing via soluble coating (transfer to the corresponding soluble counterpart via coating or coagulation with soluble particles). A dash (–) indicates the pathway is not applicable to that mode. "Speciated" contains all speciated organic and inorganic aerosol.

Mode	**Species**	**Emiss.**	**Nucl.**	**Grow./Evap.**	**Coag.**	**Coat.**
Soluble						
Nucleation	speciated	–	x	x	–	–
Aitken	BC, speciated	POA, SO_4	–	x	x	x
Accumulation	SS, BC, speciated	POA, SO_4, SS	–	x	x	x
Small coarse	SS, BC, DU, speciated	SS	–	x	x	x
Coarse	SS, BC, DU, speciated	SS	–	x	x	x
Insoluble						
Aitken	BC	BC	–	–	–	–
Accumulation	BC	BC	–	–	x	–
Small coarse	DU	DU	–	–	x	–
Coarse	DU	DU	–	–	x	–

Second, we provide a table of sector-specific anthropogenic emissions and the mapping to the

respecitive modes (same for all setups), along with the emission median diameter (Table 2 here).

Table 2: (Table S1 of the revised supplement) Primary emissions of anthropogenic aerosol subdivided by sector: Emission-to-mode mapping and median emission diameters in all setups. The median emission diameters are adopted from Kohl et al., 2023, and are applied for all primary emitted species. Black carbon is emitted to the insoluble Aitken and accumulation mode, while sulfate (2.5% of SO_2 emissions following Dentener et al., 2006) and primary organic aerosol is emitted to the soluble Aitken and accumulation mode.

	Aitken		**accumulation**	
	Fraction	Diameter	Fraction	Diameter
Agriculture	-	-	100%	310 nm
Aircraft	100%	40 nm	-	-
Biomass burning	50%	130 nm	50%	130 nm
Domestic	100%	72 nm	-	-
Energy	100%	44 nm	-	-
Industry	100%	42 nm	-	-
Ship	100%	40 nm	-	-
Traffic	100%	48 nm	-	-
Waste	-	-	100%	176 nm

Third, we provide a table on the distribution of natural emissions of dust and sea salt in all three presented setup (Table 3 here).

We added to the end of Sect. 2.2.1:

"Table 2 summarizes the species and pathways associated with each mode. All speciated soluble species can form in any soluble mode, while bulk SS, BC, POA, a small fraction of sulfate, and DU are introduced via direct emission. Freshly nucleated particles enter the nucleation mode, and particles can generally grow or shrink into neighbouring modes through condensational growth or evaporation; coagulation likewise places the resulting particle in the respective larger original mode. Upon coating with soluble material or coagulation with soluble particles, insoluble particles, i. e. dust and BC, transfer to the soluble mode. Within each mode, particles are internally mixed, while the modes themselves remain externally mixed with respect to one other (more details in Pringle et al., 2010). Fig. S1 and S2 present typical particle size distributions at the surface and in the stratosphere, respectively."

In Sect. 2.2, we added:

"Size distributions for anthropogenic primary particle emissions are applied as described by Kohl et al. (2023) (see Supplementary Material Table S1). Sea salt and dust emission size distributions were adjusted to the new modal size distributions (see Sect. 2.2.1 and Table S2)."

Additionally, we slightly adjusted the wording on the peak between 800 and 1000 nm, and added references:

"Third, it better represents sea salt and dust mass emissions, which typically show a secondary local mass maximum around 1 μm (Guelle et al., 2001; Klingmüller et al., 2018), with a

Table 3: (Table S2 of the revised supplement) Primary emissions of natural aerosol: Emission-to-mode mapping and median emission diameters in the three presented setups.

			Aitken	accumulation	small coarse	coarse
sea salt	TROPO	Fraction	0.0008%	1.1%	–	98.9%
		Diameter	70 nm	516 nm		3.3 μm
	STRATO	Fraction	0.0008%	1.1%	–	98.9%
		Diameter	70 nm	516 nm		3.3 μm
	TS	Fraction	–	0.2%	15.1%	84.7%
		Diameter		300 nm	1.12 μm	3.3 μm
mineral dust	TROPO	Fraction	–	11.3%	–	88.7%
		Diameter		516 nm		1.3 μm
	STRATO	Fraction	–	11.3%	–	88.7%
		Diameter		516 nm		2.7 μm
	TS	Fraction	–	–	28.5%	71.5%
		Diameter			1.0 μm	3.3 μm

substantial amount emitted directly into the small coarse mode (15.1% of sea salt and 28.5% of dust) in the new TS setup (see Table S2)."

2. The TS setup embodies several simultaneous changes, and the attribution to emission size alone is inferred rather than demonstrated

From Table 1, TS differs from TROPO by the addition of the small coarse mode, the narrowing of the accumulation mode (1400 → 800 nm, σ 1.59 → 1.4), the raising of the coarse threshold (1400 → 3200 nm, σ 2.0 → 1.7), and the re-mapped emissions. Importantly, "evaporation of particles into smaller than the original modes was prohibited" (l. 207–209). This is a global modification to cloud-processed aerosol release that potentially, independently reduces fine-mode primary aerosol and its long-range transport. The authors recognize the confounding in the sea salt case, but the stratospheric result is attributed to emission size alone. More analysis and discussion are helpful here.

We agree with the referee, that the resulting changes do not necessarily need to result from the size changes alone. The three simulation setups were identical with only the following three changes: Size distribution, emission-to-mode mapping, and the cloud-processing. Size distribution and emission-mode mapping changes can only be considered together. To separate the changes due to size distributions/emission from the changes due to the adjusted cloud-processing, we performed an additional simulation with the TS size setup, but without the cloud-processing adjustments, and subsequently calculated the change in the original TS simulation relative to the simulation without the adjustment to the cloud processing.

Relative changes in the speciated aerosol concentrations due to the adjusted cloud processing are illustrated in Fig. 1 (added to the supplement). It is apparent that the long-range transport is significantly suppressed, as concentrations far away from the sources strongly decrease, with the exception of ammonium and sulfate. This reduction in long-range transport is to be expected, as particles are not allowed to shrink after cloud processing anymore, and thereby sediment

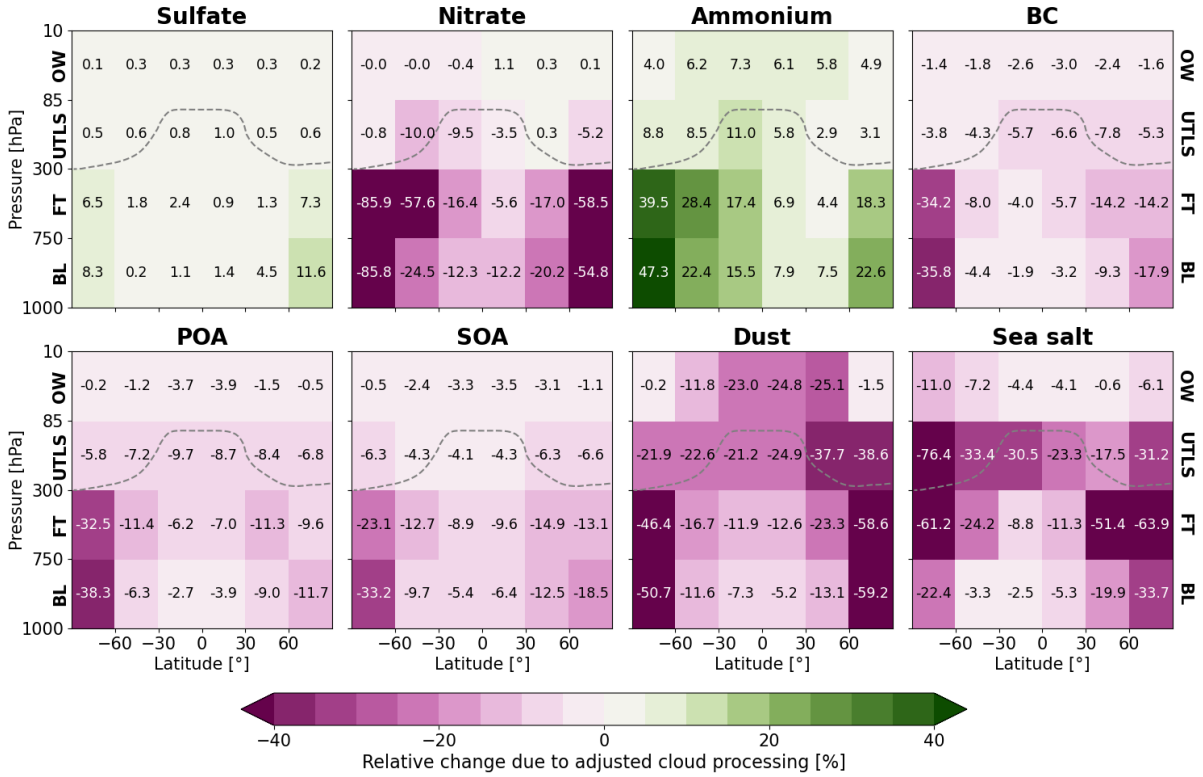


Figure 1: Change in speciated aerosol mass concentrations in the lower/middle atmosphere (2017) in the TS simulation relative to a similar simulation without the adjustments in cloud processing. Particularly, transfer to smaller modes after cloud evaporation was prohibited in the TS setup (see Sect. 2.2 of the main text).

faster. Stratospheric concentrations only exceed 10% relative changes for sea salt and dust (even up to 25% for dust in the tropical stratosphere). Thus, the adjustment of the cloud processing significantly contributes to the reduction of stratospheric dust concentrations. This is in contradiction to the sole attribution of the stratospheric dust reduction to the (emission) size distribution changes. We thank the referee for initiating a reanalysis of this effect.

Table 4 here, which we also added to the supplement of the manuscript, quantifies the effect of cloud adjustment when numerical results are compared to the observations. Note, that the metrics were adjusted to the arcsinh transformation (see reply to referee 1, including the new color scheme: relatively better (green), intermediate (orange) and worse (red) performance; see revised manuscript and reply to referee 1 for more details). While most of the species are only slightly affected ($\sim$ 10%), chloride, sodium and nitrate (affected by sea salt; see later comments) are strongly reduced by the cloud-processing. As effective shrinking after cloud evaporation was allowed in the TROPO and STRATO simulations, sea salt was further transported over continents, which is strongly reduced now.

We adjusted the sea salt discussion in the revised manuscript:

" The representation of sea salt sodium and chloride is significantly improved in the TS setup. However, sea salt concentrations remain overestimated relative to observations. A detailed comparison between modelled sea salt and reanalysis data from CAMS (Inness et al., 2019)

Table 4: (Table S3 of the revised supplement) Summary of annually averaged (2017) observed (Obs; GHOST database; Bowdalo et al., 2024) surface $PM_{2.5}$ concentrations and composition, compared to EMAC simulations using the TS setup with and without adjusted cloud processing. The number of available observational stations is indicated by N_{obs}.

	Observations		**TS**				**TS (no cloud proc. adj.)**			
	N_{obs}	Obs ($\mu g\,m^{-3}$)	$\overline{M/O}$	PF2	R^2	RMSE	$\overline{M/O}$	PF2	R^2	RMSE
NH_4^+	100	0.44	**2.16**	**37**	**0.42**	**1.01**	**1.93**	**41**	**0.42**	**0.93**
SO_4^{2-}	238	0.8	**1.48**	**73**	**0.35**	**0.61**	**1.36**	**82**	**0.42**	**0.54**
NO_3^-	237	0.57	**1.96**	**45**	**0.53**	**0.95**	**2.76**	**31**	**0.49**	**1.22**
OA	307	1.79	**1.04**	**79**	**0.34**	**0.58**	**1.18**	**74**	**0.33**	**0.59**
BC	307	0.34	**0.69**	**66**	**0.34**	**0.75**	**0.73**	**69**	**0.33**	**0.73**
Na^+	311	0.07	**3.1**	**23**	**0.62**	**1.3**	**8.67**	**3**	**0.36**	**2.29**
Cl^-	447	0.06	**9.45**	**13**	**0.14**	**2.76**	**16.67**	**7**	**0.11**	**3.24**
$PM_{2.5}$	3461	11.61	**0.9**	**90**	**0.25**	**0.47**	**1.03**	**90**	**0.25**	**0.46**

and MERRA-II (Gelaro et al., 2017; Randles et al., 2017) indicates that the applied changes reduce the long-range transport of sea salt particles to continental regions, sharpening the sea salt gradients between oceanic and continental areas compared to simulations with previously used setups. This results in substantially improved agreement with reanalysis data across all size ranges (Appendix A and Fig. A1), though we note that this comparison should be interpreted as a cross-model consistency check rather than an independent observational validation, since both reanalysis products assimilate total column AOD rather than speciated aerosol properties (see Appendix A).

To separate the effects of the adjusted (emission) size distribution from the adjustments in the re-evaporation (see Sect. 2.2), we performed a simulation with the TS setup without the adjustment to the cloud processing, i. e. allowing shrinking of particles to smaller modes after cloud re-evaporation, and compared it to the original TS simulation (Table S3). Surface concentrations affected by sea salt (sodium, chloride and nitrate) are strongly reduced due to the adjusted cloud processing in the TS setup, while most other species are barely affected ($\sim$ 10%). Thus, the prohibition of aerosol shrinking due to cloud-processing leads to strongly reduced sea salt transport over continental regions, and better agreement with observations. ”

Additionally, we reformulated the discussion on the dust reduction in Sect. 5:

” Simulations with the new TS setup reduce desert dust concentrations in the UTLS in line with recent observations (see Sect. 4), driven by two compounding changes relative to the TROPO and STRATO setups. First, in the previous setups, dust was partly emitted into the accumulation mode and, upon ageing, became internally mixed with particles that grew into this mode, averaging $\sim$200 nm diameter. This configuration effectively downscaled the typical dust size (900 nm), enhancing vertical transport and leading to overestimated stratospheric dust. Emitting desert dust into the additional small coarse mode reduces this effect (Fig. S1a). Second, the prohibition of particle shrinkage into smaller modes following cloud re-evaporation (Sect. 2.2) independently reduces long-range and vertical transport of coarse-mode particles, including dust. A sensitivity simulation without this adjustment shows that stratospheric dust

concentrations increase by up to 25% relative to the TS setup (Fig. S25), indicating that both the revised emission size distribution and the adjusted cloud-processing treatment contribute to the reduced stratospheric dust burden. Nevertheless, dust in the UTLS remains slightly overestimated. Good model agreement with observed gas-phase tracers such as CO (Fig. S17 and S18), indicates reasonably accurate vertical transport, suggesting that insufficient wet scavenging, likely due to the grid-box averaged parametrization of convective transport, is the most probable cause of the residual overestimation. "

In the conclusion, we changed the following:

" The lower abundance of primary material in the stratosphere, mostly driven by a reduction in dust concentrations, is attributed to the combined effect of a revised emission size distribution and an adjusted treatment of cloud-processed particle re-evaporation, both tailored to the new modal aerosol setup (Sect. 5). "

In Sect. 2.2, we changed:

" ... and evaporation of particles into smaller than the original modes was prohibited to better represent the transport of coarse dust and sea salt particles. This adjustment, together with the revised emission size distribution (Sect. 2.2.1), contributes to the reduced long-range transport of coarse-mode aerosol discussed in Sect. 5. "

In Sect. 4, we added:

" Primary material abundance (POA, BC, dust and sea salt mass) is limited in the stratosphere, falling below 3.5% globally in the stratospheric overworld (see Sect. 5 for a discussion of the contributing factors to this reduction). "

3. "Primary particles" is undefined, and the model and observational definitions are not commensurable

The abstract states that "primary particles contribute less than 3.5% to aerosol mass in the stratospheric overworld... in closer agreement with recent observations" (l. 10–13), but the term is defined nowhere. From Sect. 2.2 and Fig. 9 I infer it means the summed Dust, BC, POA and sea salt tracer mass; on that reading the arithmetic checks out, since summing the four primary panels of the OW row in Fig. 9 gives a maximum near 3.3%. Two issues follow.

- (a) Mass of primary material is not mass of primary particles. Modes are internally mixed, so a droplet nucleated on a dust core and grown by H_2SO_4 condensation is almost entirely secondary by mass while a single-particle instrument would classify it as dust-containing. Please state which quantity is reported.
- (b) The Sect. 4 diagnostics appear to be raw modal output, whereas Sect. 3 applies the careful sampling of Sect. 2.3. This matters concretely: TS places dust largely in the 800–3200 nm mode, outside HR-AMS transmission and at the upper edge of the PALMS range. Please either apply the Sect. 2.3 sampling where a comparison to observations is claimed, or state that Sect. 4 reports unfiltered output and adjust the abstract. Minor but related: the species in Fig. 9 sum to ∼100% per cell, indicating that particle-bound water is

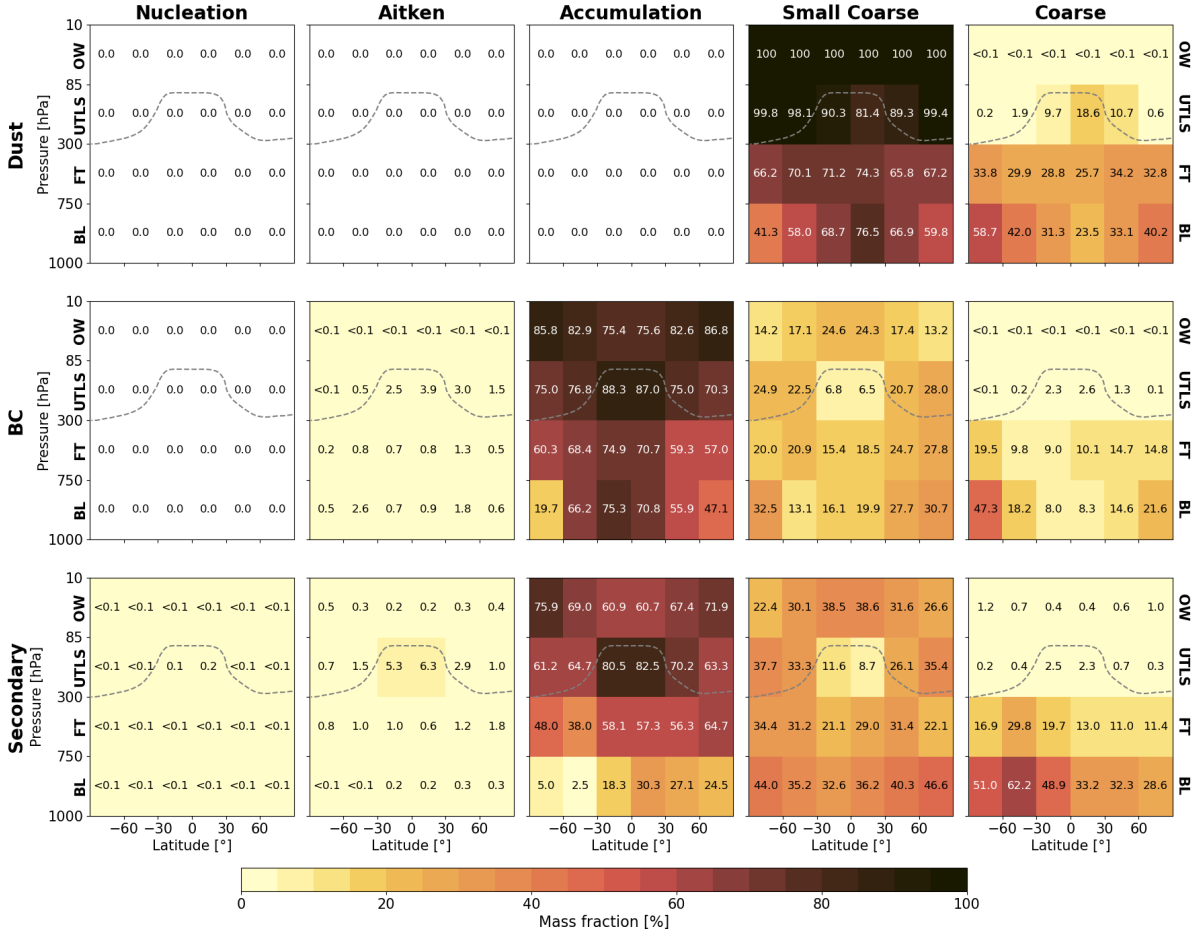


Figure 2: Fractional contribution of each mode to Dust, BC and secondary mass in the different atmospheric domains (2017).

excluded. Given that the manuscript repeatedly describes deliquesced sulfate droplets, please state this convention explicitly.

We fully agree with the referee on this point. The term "primary particles" refers to the sum of dust, BC, POA and sea salt tracer mass which are directly emitted and not chemically formed. We apologize for not defining it thoroughly.

- (a) This means, based on our definition, that we refer to "primary material" rather than "primary particles". We correct this in the manuscript, and state all text changes below. The exact inference of the number of primary particles is not possible in our model after aerosol ageing in the atmosphere.
- b) We partly agree here. Sect. 4 is the raw model output, yes. However, the dust comparison is not using HR-AMS observations, but rather a combination of the PALMS instrument, and the aerosol microphysical properties (AMP) suite, extending up to 4.8 μm. This also includes the dust emission modes at 1.0 and 3.3 μm. We now state the following in line 512: "Note that no size cuts have been performed throughout this section, and unfiltered dry PM mass concentrations (excluding aerosol water) are shown." Further, we argue that in the stratospheric overworld coarse dust particles are barely relevant, as dust is only transported to the stratospheric overworld in the small coarse mode (800-3200

nm), which is well covered by the PALMS observational size range. We show this in Fig. 2, which we additionally added to the revised supplement. We also added the following sentence to the revised manuscript: "Fig. S23 shows, that UTLS and stratospheric dust concentrations are strongly dominated by the small coarse mode, even though more mass is emitted into the coarse mode."

Additional text changes:

L9 (abstract): "Primary emitted aerosol mass contributes less than 3.5% in the stratospheric overworld up to 10 hPa, substantially less than suggested by previous modelling studies and in closer agreement with recent observations."

L466: "Both campaigns observed low concentrations of primary particles, especially with dust and BC composition, in the ATAL (e.g., Appel et al., 2022; Berberich et al., 2025; Ebert et al., 2024). The model successfully reproduces these low UTLS BC mass concentrations, with values below 10 ng m^{-3}."

L540: "Primary material abundance (POA, BC, dust and sea salt mass) is limited in the stratosphere, falling below 3.5% globally in the stratospheric overworld."

L643: "We find that primary material contributes less than 3.5% to aerosol mass in the stratospheric overworld, significantly lower than reported by previous model studies, and more consistent with recent observations. The lower abundance of primary material in the stratosphere is attributed ..."

4. The 3.5% is mainly carried by POA, but the claim is all about dust

In the overworld row of Fig. 9, POA contributes 1.7–3.0%, BC ≤0.3%, dust ≤0.7% and sea salt <0.1%. Primary organic aerosol accounts for roughly four fifths of the primary mass; dust for well under a quarter. Sect. 5 (l. 596–605) and the Conclusions (l. 645) explain the low primary fraction entirely through the revised dust emission size. That mechanism addresses the smaller component, and it is not obvious that it affects POA transport at all, since POA is not emitted at the sizes that motivated the new mode. This is compounded by the authors' own statement that "these factors likely contribute to an overestimation of OA in the FT" (l. 594). Please discuss what controls POA transport into the overworld, how it differs between setups, and whether the known FT overestimate propagates.

The referee is correct, that the changes to the emission size distribution only affect dust and sea salt, and not BC and POA, as these are emitted in the Aitken and accumulation mode, not directly affected by these changes. Further, the observational constraints are mostly related to dust. However, this does not contradict our statement. It is true, that primary particles are mostly dominated by POA in the TS setup. In the TROPO and STRATO setup, however, primary mass in the stratospheric overworld was dominated by dust. We apologize for not further clarifying this.

We illustrate this in Fig. 3, which we also provide in the revised supplement. The fraction of primary material in the tropical stratosphere reduced from up to ∼ 6% (TROPO) and ∼ 9% (STRATO) to below 3% due to the model improvements. This is almost entirely attributable to the dust contribution changes in the stratospheric overworld, which is reduced by a factor

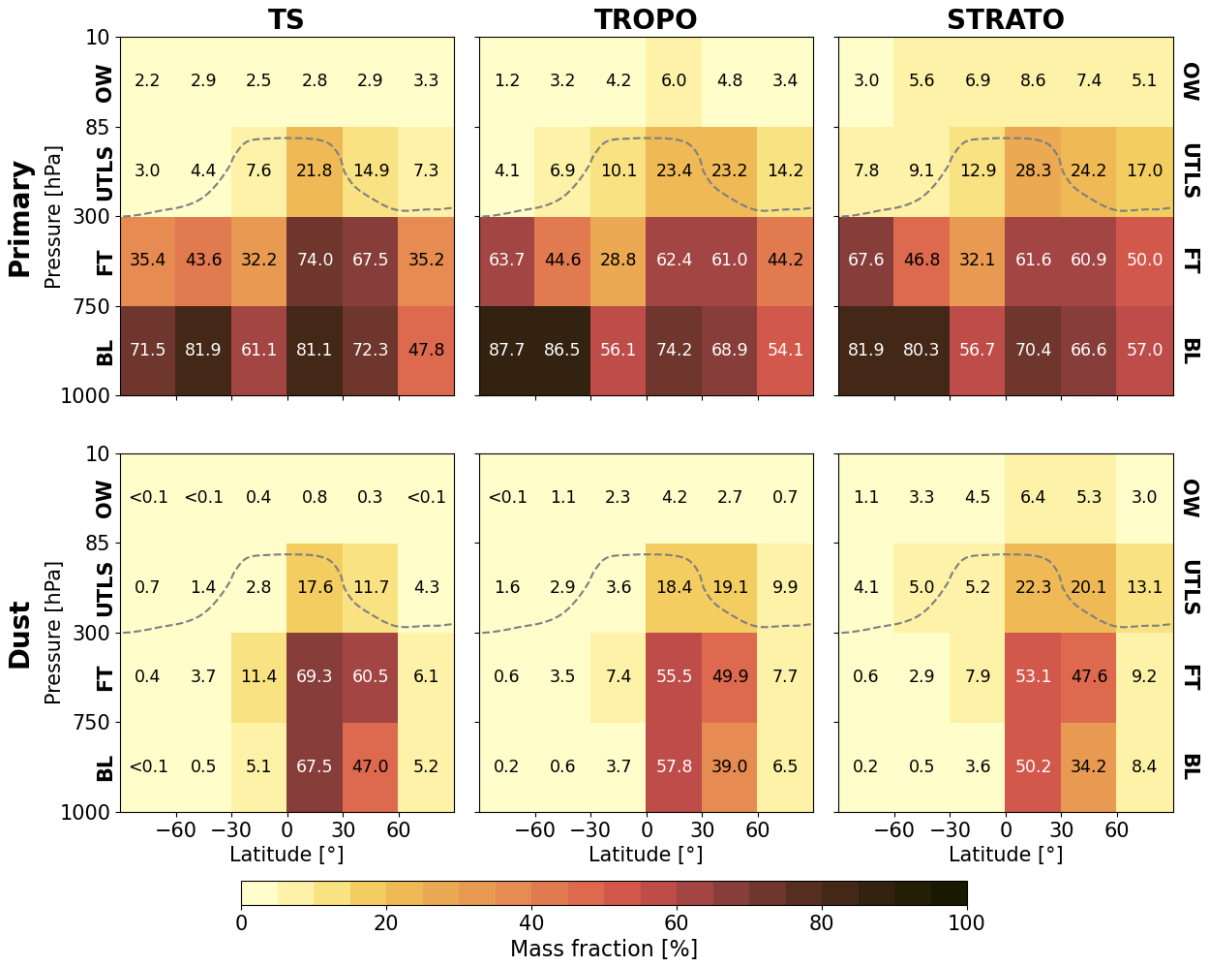


Figure 3: Zonally and multi-annually (2016-2019) averaged simulated mass fraction of total primary material (top) and mineral dust (bottom) for the three simulation setups (TS, TROPO and STRATO).

of 5 to 10. So even though POA is now dominating, the decrease in primary mass is due to the changes in dust.

We would like to clarify that POA does not drive the reduction in primary material between setups. The contribution of POA to the total aerosol mass remains relatively stable throughout the stratospheric overworld among the three setups ($\sim 1.7 - 3.0\%$ in the OW). It is now the dominating primary species, as it is emitted at smaller sizes than dust and sea salt, but at greater magnitude than BC.

We added the following sentence to the discussion in Sect. 4 in the revised manuscript:

" While the reduction in primary material compared to the TROPO and STRATO simulations is driven almost entirely by dust (Fig. S21), the remaining fraction in the stratospheric overworld is dominated by POA due to the smaller emissions size relative to dust and larger emission magnitude relative to BC. "

We acknowledge that the known tendency toward free-tropospheric OA overestimation (Sect. 5) may, in principle, propagate upward into this residual POA contribution via convective and slow ascent transport. Thus, we have added to the discussion in Sect. 5 (see also next

comment):

" We acknowledge that this bias in OA may also lead to an overestimation of POA and SOA in the UTLS and stratospheric overworld (see above). As ORACLE neglects both the Kelvin effect and kinetic limitations on condensation, which would otherwise suppress SOA uptake onto the limited aerosol surface area available in the UT and UTLS, the reported SOA fractions in this region likely represent an upper bound rather than a precisely constrained estimate. However, model-observation agreement for OA improves toward the UTLS (e.g., Fig. 6, near the upper boundary of the ATAL). "

5. The tropical UTLS SOA fraction

Figure 9 shows SOA mass fractions of 63.6% (30°S–0°) and 43.7% (0–30°N) in the UTLS, against sulfate fractions near 23.5%. The abstract instead quotes 15%, corresponding to the overworld row. A tropical UTLS that is SOA-dominated rather than sulfate-dominated is considerably consequential for heterogeneous chemistry, optical properties, and the common modelling assumption of a sulfuric acid–water aerosol. Discussion about its importance is absent. I assume the results depend heavily on ORACLE, which the authors note "does not account for the Kelvin effect and the kinetic limitations in condensation" (l. 588–589). Please give an uncertainty range on the reported SOA fractions.

The high percentages (63.6% (30°S–0°) and 43.7% (0–30°N)) refer to the tropical UT. The abstract on the other hand refers to the "global lower stratosphere", not the UTLS in general. It is important to separate the UTLS here into the tropical UT and the extratropical lowermost stratosphere (ExLS). The tropical UT is indeed dominated by SOA, while the influence decreases towards the ExLS, which is dominated by sulfate. The lower tropical stratosphere also has a SOA fraction of $\lesssim$ 13% (note, that this was corrected to 13% as the numbers slightly changed, when considering the complete time frame from 2016 to 2019). So when referring to the global lower stratosphere, meaning 300 to 85 hPa at higher latitudes and 85 to 10 hPa in the tropics, we consider our wording in the abstract correct.

Recent observations actually showed this band of organic particles in the lowermost stratosphere (Lyu et al., 2026), in accordance with our simulations. So the lower stratosphere is still dominated by sulfate, but with some significant organic additions, that sure have implications for heterogeneous chemistry and the aerosol state in the stratosphere. To give a quantitative uncertainty range is not really possible based on the model simulations, but we discuss qualitative uncertainties in the "Discussion & Limitations" section, now with an explicit cross-reference to stratospheric SOA (see previous reply).

To summarize: The tropical UT(LS) is dominated by SOA; this is not itself a new result of our study. The stratospheric overworld, which is more commonly represented by the standard sulfuric acid–water assumption in modelling and remote sensing, remains sulfate-dominated in our simulations, with a secondary but non-negligible ($\lesssim$ 13%) organic contribution, consistent with the very recent independent findings of Lyu et al., 2026.

We shortly add to the conclusions in the revised manuscript:

" SOA contributes $\lesssim$ 13% to the tropical stratospheric aerosol burden, but declines sharply with altitude, in line with recent observations (Lyu et al., 2026), forming a tropical band throughout the UTLS. While sulfate remains the dominant aerosol component in the stratospheric

overworld, this non-negligible organic contribution may have implications for the heterogeneous chemistry and optical properties of stratospheric aerosol relative to the standard sulfuric acid–water assumption, requiring further dedicated investigation. ”

6. Three problems cluster in the southern extratropics

The manuscript documents underestimated SAOD at southern mid-to-high latitudes with the cause left open (l. 502–503, Fig. 7). Substantial underestimation of sulfate, ammonium, OA, BC and BL PNC over the Southern Ocean (Fig. 4 bottom row) and an annual-mean nitrate fraction of 54.2% in the southern polar overworld (Fig. 9, l. 538–539). Given the overlapping regions and that the first two are both consistent with missing aerosol mass, please discuss them jointly in Section 5.

We thank the referee for raising this point, as it connects some model-observational discrepancies to similar causes. The underestimation of sAOD at intermediate to high southern latitudes is very likely connected to the underestimation of mass in comparison to ATom, and this should definitely be considered together. The high nitrate fraction above 60°S stems from PSCs, however, does not directly affect the sAOD range between 45 and 60°S. Whether the underestimation of BL PNC is connected to the issue at higher altitudes, is unclear, and would be speculative without further evidence. For that reason, we do not consider this together. We have made the following text additions:

In the discussion of the underestimated sAOD in Sect. 3.4, we added the following sentence instead of ”Whether this discrepancy reflects underestimated aerosol sources or deficiencies in the representation of relevant transport and microphysical processes remains unclear.”:

” This underestimation coincides with the underestimated tropospheric aerosol mass found over the Southern Ocean and South Pacific in comparison to ATom observations (Sect. 3.3.1), and is discussed jointly with that finding in Sect. 5. The wintertime peak in sAOD at southern mid-latitudes (45–60°S) is visible in OMPS-LP at 746 nm but not consistently reproduced across instruments or by the model (Fig. 7); possible explanations are discussed in Sect. 5. ”

In Sect. 5, we discuss this after the general discussion of sulfate underestimation:

” Largest uncertainties arise in mid- to high southern latitudes, where the sulfate (and associated aerosol mass) underestimation discussed above is most pronounced (Sect. 3.3.1; Appendix B). This deficit likely contributes to the underestimated sAOD at southern mid-latitudes (Sect. 3.4, Fig. 7). Separately, the elevated annual-mean nitrate mass fraction in the southern polar stratospheric overworld (poleward of 60°S; Sect. 4, Fig. 9) reflects heterogeneous nitric acid uptake into ternary/PSC-related liquid solutions (MSBM submodel, Sect. 2.2). This nitrate-associated mass is not currently included in the AOP optical property calculations (Sect. 2.2) and therefore does not contribute to simulated extinction, likely explaining part of the sAOD underestimation specifically at the highest southern latitudes (see Fig. S22). The more localized sAOD underestimation at 45–60°S during austral winter at 750 nm, occurs equatorward of the region where nitrate dominates aerosol composition in our annual-mean simulations, and is not consistently reproduced across independent satellite products (Fig. 7, OMPS-LP observations). Whether this discrepancy is an observational artefact or the result from a real physical phenomenon, such as extensions of PSCs to lower latitudes or diabatic descent of meteoric material (see below), remains unclear. ”

Specific comments

2.2, l. 176–184. Please add an explicit definition of primary vs. secondary aerosol as used here, with the species list.

We added the following sentence to the end of the paragraph:

"POA, BC, DU and SS are directly emitted into the lower atmosphere (primary aerosol), whereas all other species form secondary in the atmosphere or condense onto pre-existing particles."

Sect. 2.2.1, l. 231–237. The mode descriptions are qualitative. Please state, for each mode, which species it can contain and by which route they arrive — direct emission, nucleation, growth across the boundary from the mode below, intermodal coagulation, or insoluble-to-soluble ageing. This would resolve much of M1 in a few sentences.

We agree, that the mode descriptions were qualitative in the submitted manuscript. For that reason, we provided the three Tables 1, 2, 3, discussed in M1 (see above). These tables provide information, which modes contains which species (Table 1) and which emissions are distributed to which modes (Tables 2 and 3).

We added to the end of Sect. 2.2.1 (see above):

"Table 2 summarizes the species and pathways associated with each mode. All speciated soluble species can form in any soluble mode, while SS, BC, POA, a small fraction of sulfate, and DU are introduced via direct emission. Freshly nucleated particles enter the nucleation mode, and particles generally grow into the next larger mode through condensational growth; coagulation likewise places the resulting particle in the respective larger original mode. Upon coating with soluble material or coagulation with soluble particles, insoluble particles, i. e. dust and BC, transfer to the soluble mode. Within each mode, particles are internally mixed, while the modes themselves remain externally mixed with respect to one other."

Table 1. Please state the total number of modes per configuration (7, 7 and 9, if I understand correctly) and indicate which modes have insoluble counterparts.

We adjusted the caption of Table 1 of the submitted manuscript as follows:

" Modal size distribution in the new setup for the entire lower and middle atmosphere (TS; 9 modes used in this study) in comparison to size distributions used in earlier studies, which focussed either on the troposphere (TROPO; 7 modes) or the stratosphere (STRATO; 7 modes). The *small coarse mode* was added between the accumulation and the coarse mode in the TS setup. All soluble modes have an insoluble counterpart, except for the nucleation mode, as no insoluble material can enter the nucleation mode (see also Table S3). The median diameter can adjust within the given diameter boundaries. Additionally, the globally constant sigma of the log-normal distribution is given for each mode. "

Table 2. The improvements in Na^+ (M/O 17.59 $\rightarrow$ 6.08 $\rightarrow$ 3.0), Cl^- (30.16 $\rightarrow$

10.09 → 7.55) and NO_3^- (4.77 → 3.05 → 1.96) are substantial and well presented. However sulfate is worse in TS than in TROPO on every metric (M/O 1.48 vs. 1.18; PF2 73 vs. 88; R^2_{log} 0.35 vs. 0.54), and total $PM_{2.5}$ is essentially tied. The text at l. 313–316 reports the nitrate improvement but not this. Acknowledging it would strengthen the paper.

We agree with the referee, and apologize for not discussing this. We adjusted the first sentence of the paragraph to:

" The TS and TROPO simulations exhibit comparable performance in predicting surface mass concentrations of key aerosol species (see Table 2), confirming the suitability of the TS setup for surface-level studies, with only sulfate showing worse agreement with observations compared to the TROPO setup. "

Fig. 2. Chloride remains overestimated with $R^2_{log} = 0.17$ even in TS. Some discussion of why Cl^- specifically remains poor would be welcome.

Chloride concentrations over continents originating from sea salt are affected by two main processes: transport and thermodynamics. While sodium mostly stays in the aerosol phase, chloride can escape to the gas phase via the two acid displacement reactions:

$$HNO_3(g) + NaCl_{(aq)} \rightleftharpoons NaNO_{3(aq)} + HCl(g) \tag{1}$$

and

$$H_2SO_4(g) + 2NaCl_{(aq)} \rightleftharpoons Na_2SO_{4(aq)} + 2HCl(g). \tag{2}$$

So while sea-salt transport (and thus sodium) is substantially improved compared to the other setups, chloride remains more strongly biased because its particulate abundance additionally depends on these displacement reactions. Since chloride is overestimated in the model, this indicates that the simulated displacement/depletion is too week relative to observations. This is supported by Fig. 4, which compares simulated and observed sodium, chloride, and nitrate concentrations globally: the observed marine-to-continental gradient is already stronger for chloride than for sodium (consistent with chloride depletion during transport), whereas this gradient is underestimated in the model.

Additionally, the co-located overestimation of ammonium at the surface may promote excess ammonium chloride formation, further contributing to the bias.

We discuss this shortly in the evaluation of the revised manuscript (together with the changes due to a similar comment by referee 1). We added the following sentences:

" The overestimation in NO_3^- concentrations in the TROPO and STRATO simulations, also present in earlier evaluations using the TROPO modal setup (e.g., Pozzer et al., 2022), is significantly reduced in the TS setup, although a residual overestimation remains. This behavior is closely linked to the sea salt sodium and chloride bias (see above): unlike sodium, which remains almost entirely in the particulate phase, chloride can be lost to the gas phase via acid displacement reactions with nitric and sulfuric acid (e. g., $HNO_3(g) + NaCl_{(aq)} \rightleftharpoons NaNO_{3(aq)} + HCl(g)$), shifting the ISORROPIA-II thermodynamic equilibrium toward particulate nitrate formation. This chloride depletion process is well documented observationally (Dasgupta et al., 2007; Gard

et al., 1998; Guimbaud et al., 2002; Su et al., 2022) and typically produces a stronger marine-to-continental gradient for chloride than for sodium (Fig. S4). Our simulations reproduce this gradient only partially, consistent with the matching cross-setup ranking of sea salt and NO_3^- overestimation (Table 3), and indicating that the model underestimates the extent of chloride depletion during transport. The co-located overestimation of ammonium (Fig. 2) may additionally promote excess ammonium chloride formation, further contributing to the chloride bias. An additional complicating factor is that ISORROPIA-II assumes instantaneous equilibrium for the entire particle, which is less justified for the (comparatively coarse) sea-salt-dominated modes, where in reality only the particle surface interacts with the gas phase. "

Fig. 4. **The detection-limit band overlaps much of the upper-altitude comparison. Please state what fraction of UTLS observations lie below detection.**

We thank the referee for this question, but do not agree, that most of the upper-altitude comparison is covered by the detection limit. We would first like to clarify a related point: the grey shaded area in Fig. 4 indicates the altitude-averaged instrument detection limit, whereas the pink area separately marks the linear range of the symlog x-axis scaling (used purely for visualization of near-zero values) and does not represent a detection limit; we agree these two shaded regions may be easily confused and have slightly adjusted the figure caption accordingly (see below). Quantitatively, above 8 km (roughly covering the lower part of the UTLS region), only a minor fraction of the region-season-altitude medians used for the statistical comparison (Table 3) fall below the respective instrument detection limit: ammonium 18.5%, nitrate 11.2%, organic aerosol 0.7%, and sulfate and dust 0.0%. No detection limit is defined for BC or PNC observations. We therefore conclude that the model-observation comparison shown in Fig. 4 above 8 km is not substantially affected by instrument detection limits."

Text addition in the discussion of Fig. 4 and Table 3:

"The fraction of region-season-altitude medians used for the statistical comparison (Table 3) that fall below the respective instrument detection limit remains small throughout the profile, slightly increasing from the BL toward the UTLS for species present at low ambient concentrations (ammonium: 18.5%; nitrate: 11.2%), while remaining negligible for OA, sulfate, and dust ($\leq$0.7%; no detection limit is defined for BC or PNC)."

Adjustment to the caption of Fig. 4:

"Grey shaded area indicates the altitude-averaged detection limit of the instrument; the pink area separately marks the linear range of the symlog x-axis scaling and does not represent a detection limit."

Fig. 7. **Please state whether omitting pyroconvective stratospheric injection (e.g. the unreproduced August 2017 event) affects the annual-mean POA and BC fractions in Sect. 4 and 5.**

We thank the referee for pointing that out, as we failed to discuss this. In fact, inclusion of strong wildfires that reach the stratosphere will affect the stratospheric fraction of POA and BC. We now discuss this in Sect. 4 and 5, and shortly in the conclusions.

Sect. 4 addition:

"We note that this estimate does not include direct stratospheric injection of smoke by pyroconvective wildfire events, which are not resolved in the current simulations (see also Sect. 3.4

and 5) and can locally and episodically enhance the BC and POA fraction of the stratospheric aerosol burden."

Sect. 5 addition:

"The reported stratospheric mass fractions (Sect. 4) exclude direct stratospheric injection of biomass burning smoke via pyroconvection. As shown in Sect. 3.4 (Fig. 7), the simulations do not reproduce the sAOD enhancement observed at northern midlatitudes in August 2017, attributed to the British Columbia wildfires (Brühl et al., 2025; Healy et al., 2019), nor other documented pyroCb events known to inject smoke directly into the stratosphere (e. g., Ditas et al., 2018; Katich et al., 2023; Ma et al., 2024). Such events can episodically but substantially increase the stratospheric BC and POA fraction in affected regions and seasons (Brühl et al., 2025). The annual-mean fractions reported in Sect. 4 should therefore be considered a lower bound, not representative of years with more frequent or intense wildfire activity. Incorporating pyroconvective injection in standard EMAC simulations is a priority for future model development."

Conclusion addition:

"We find that primary material contributes less than 3.5% to aerosol mass in the stratospheric overworld, significantly lower than reported by previous model studies, and more consistent with recent observations. This estimate excludes direct pyroconvective injection of biomass burning smoke, an episodic but potentially significant source not resolved in the current simulations (Sect. 5), and should therefore be considered a lower bound rather than a complete accounting of primary carbonaceous aerosol in the stratosphere."

Fig. 9. **Consider adding a "primary total" panel so the 3.5% can be read directly rather than reconstructed from four panels.**

We thank the referee for this suggestion. We now added Fig. 3 here to the supplement, providing the suggested figure.

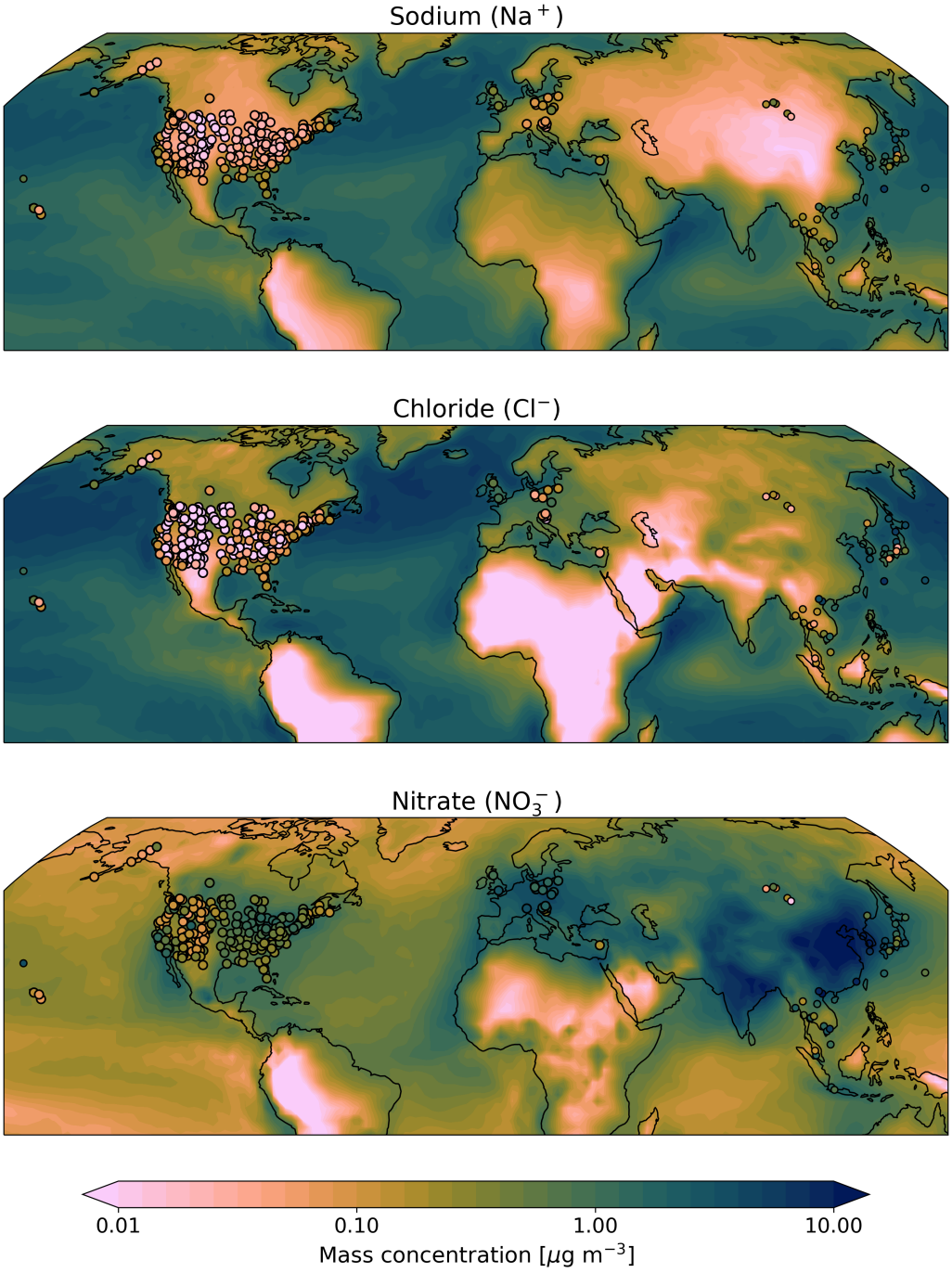


Figure 4: Simulated mass concentrations of sodium (top), chloride (middle) and nitrate (bottom), overlayed with observations from the GHOST dataset.

References

Appel, O., F. Köllner, A. Dragoneas, A. Hünig, S. Molleker, H. Schlager, C. Mahnke, R. Weigel, M. Port, C. Schulz, F. Drewnick, B. Vogel, F. Stroh, and S. Borrmann (2022). "Chemical analysis of the Asian tropopause aerosol layer (ATAL) with emphasis on secondary aerosol particles using aircraft-based in situ aerosol mass spectrometry". *Atmospheric Chemistry and Physics* 22.20, pp. 13607–13630. DOI: 10.5194/acp-22-13607-2022.

Berberich, J., S. A. Jacoby, G. Michailoudi, J. P. Schwarz, S. Viciani, F. D'Amato, G. Bianchini, M. Barucci, T. Campos, K. Ullman, J. R. Podolske, C. Gurganus, W. P. Smith, R. Ueyama, S. B. Honomichl, L. L. Pan, S. Woods, B. Wienzierl, M. Dollner, and A. E. Perring (2025). "Black Carbon Reflects Extremely Efficient Aerosol Wet Removal in Monsoonal Convective Transport". *Journal of Geophysical Research: Atmospheres* 130.3, e2024JD042692. DOI: 10.1029/2024JD042692.

Bowdalo, D., S. Basart, M. Guevara, O. Jorba, C. Pérez García-Pando, M. Jaimes Palomera, O. Rivera Hernandez, M. Puchalski, D. Gay, J. Klausen, S. Moreno, S. Netcheva, and O. Tarasova (2024). "GHOST: a globally harmonised dataset of surface atmospheric composition measurements". *Earth System Science Data* 16.10, pp. 4417–4495. DOI: 10.5194/essd-16-4417-2024.

Brühl, C., M. Kohl, and J. Lelieveld (2025). "Radiative forcing and stratospheric ozone changes due to major forest fires and recent volcanic eruptions including Hunga Tonga". *Atmospheric Chemistry and Physics* 25.24, pp. 18697–18718. DOI: 10.5194/acp-25-18697-2025.

Dasgupta, P. K., S. W. Campbell, R. S. Al-Horr, S. R. Ullah, J. Li, C. Amalfitano, and N. D. Poor (2007). "Conversion of sea salt aerosol to NaNO3 and the production of HCl: Analysis of temporal behavior of aerosol chloride/nitrate and gaseous HCl/HNO3 concentrations with AIM". *Atmospheric Environment* 41.20. (BRACE), pp. 4242–4257. ISSN: 1352-2310. DOI: j.atmosenv.2006.09.054.

Dentener, F., S. Kinne, T. Bond, O. Boucher, J. Cofala, S. Generoso, P. Ginoux, S. Gong, J. J. Hoelzemann, A. Ito, L. Marelli, J. E. Penner, J.-P. Putaud, C. Textor, M. Schulz, G. R. van der Werf, and J. Wilson (2006). "Emissions of primary aerosol and precursor gases in the years 2000 and 1750 prescribed data-sets for AeroCom". *Atmospheric Chemistry and Physics* 6.12, pp. 4321–4344. DOI: 10.5194/acp-6-4321-2006.

Ditas, J., N. Ma, Y. Zhang, D. Assmann, M. Neumaier, H. Riede, E. Karu, J. Williams, D. Scharffe, Q. Wang, J. Saturno, J. P. Schwarz, J. M. Katich, G. R. McMeeking, A. Zahn, M. Hermann, C. A. M. Brenninkmeijer, M. O. Andreae, U. Pöschl, H. Su, and Y. Cheng (2018). "Strong impact of wildfires on the abundance and aging of black carbon in the lowermost stratosphere". *Proceedings of the National Academy of Sciences* 115.50, E11595–E11603. DOI: 10.1073/pnas.1806868115.

Ebert, M., R. Weigel, S. Weinbruch, L. Schneider, K. Kandler, S. Lauterbach, F. Köllner, F. Plöger, G. Günther, B. Vogel, and S. Borrmann (2024). "Characterization of refractory aerosol particles collected in the tropical upper troposphere–lower stratosphere (UTLS) within the Asian tropopause aerosol layer (ATAL)". *Atmospheric Chemistry and Physics* 24.8, pp. 4771–4788. DOI: 10.5194/acp-24-4771-2024.

Gard, E. E., M. J. Kleeman, D. S. Gross, L. S. Hughes, J. O. Allen, B. D. Morrical, D. P. Fergenson, T. Dienes, M. E. Gälli, R. J. Johnson, G. R. Cass, and K. A. Prather (1998). "Direct Observation of Heterogeneous Chemistry in the Atmosphere". *Science* 279.5354, pp. 1184–1187. DOI: 10.1126/science.279.5354.1184.

Gelaro, R., W. McCarty, M. J. Suárez, R. Todling, A. Molod, L. Takacs, C. A. Randles, A. Darmenov, M. G. Bosilovich, R. Reichle, K. Wargan, L. Coy, R. Cullather, C. Draper, S. Akella, V. Buchard, A. Conaty, A. M. da Silva, W. Gu, G.-K. Kim, R. Koster, R. Lucchesi, D. Merkova, J. E. Nielsen, G. Partyka, S. Pawson, W. Putman, M. Rienecker, S. D. Schubert, M. Sienkiewicz, and B. Zhao (2017). "The Modern-Era Retrospective Analysis for Research and Applications, Version 2 (MERRA-2)". *Journal of Climate* 30.14, pp. 5419–5454. DOI: 10.1175/JCLI-D-16-0758.1.

Guelle, W., M. Schulz, Y. Balkanski, and F. Dentener (2001). "Influence of the source formulation on modeling the atmospheric global distribution of sea salt aerosol". *Journal of Geophysical Research: Atmospheres* 106.D21, pp. 27509–27524. DOI: 10.1029/2001JD900249.

Guimbaud, C., F. Arens, L. Gutzwiller, H. W. Gäggeler, and M. Ammann (2002). "Uptake of HNO_3 to deliquescent sea-salt particles: a study using the short-lived radioactive isotope tracer ^{13}N". *Atmospheric Chemistry and Physics* 2.4, pp. 249–257. DOI: 10.5194/acp-2-249-2002.

Healy, R. M., J. M. Wang, U. Sofowote, Y. Su, J. Debosz, M. Noble, A. Munoz, C.-H. Jeong, N. Hilker, G. J. Evans, and G. Doerksen (2019). "Black carbon in the Lower Fraser Valley, British Columbia: Impact of 2017 wildfires on local air quality and aerosol optical properties". *Atmospheric Environment* 217, p. 116976. ISSN: 1352-2310. DOI: 10.1016/j.atmosenv.2019.116976.

Inness, A., M. Ades, A. Agusti-Panareda, J. Barré, A. Benedictow, A.-M. Blechschmidt, J. J. Dominguez, R. Engelen, H. Eskes, J. Flemming, V. Huijnen, L. Jones, Z. Kipling, S. Massart, M. Parrington, V.-H. Peuch, M. Razinger, S. Remy, M. Schulz, and M. Suttie (2019). "The CAMS reanalysis of atmospheric composition". *Atmospheric Chemistry and Physics* 19.6, pp. 3515–3556. DOI: 10.5194/acp-19-3515-2019.

Katich, J. M., E. C. Apel, I. Bourgeois, C. A. Brock, T. P. Bui, P. Campuzano-Jost, R. Commane, B. Daube, M. Dollner, M. Fromm, K. D. Froyd, A. J. Hills, R. S. Hornbrook, J. L. Jimenez, A. Kupc, K. D. Lamb, K. McKain, F. Moore, D. M. Murphy, B. A. Nault, J. Peischl, A. E. Perring, D. A. Peterson, E. A. Ray, K. H. Rosenlof, T. Ryerson, G. P. Schill, J. C. Schroder, B. Weinzierl, C. Thompson, C. J. Williamson, S. C. Wofsy, P. Yu, and J. P. Schwarz (2023). "Pyrocumulonimbus affect average stratospheric aerosol composition". *Science* 379.6634, pp. 815–820. DOI: 10.1126/science.add3101.

Klingmüller, K., S. Metzger, M. Abdelkader, V. A. Karydis, G. L. Stenchikov, A. Pozzer, and J. Lelieveld (2018). "Revised mineral dust emissions in the atmospheric chemistry–climate model EMAC (MESSy 2.52 DU_Astitha1 KKDU2017 patch)". *Geoscientific Model Development* 11.3, pp. 989–1008. DOI: 10.5194/gmd-11-989-2018.

Kohl, M., J. Lelieveld, S. Chowdhury, S. Ehrhart, D. Sharma, Y. Cheng, S. N. Tripathi, M. Sebastian, G. Pandithurai, H. Wang, and A. Pozzer (2023). "Numerical simulation and evaluation of global ultrafine particle concentrations at the Earth's surface". *Atmospheric Chemistry and Physics* 23.20, pp. 13191–13215. DOI: 10.5194/acp-23-13191-2023.

Lyu, M., A. T. Ahern, G. P. Schill, M. J. Lawler, D. M. Murphy, S. J. Taylor, A. Fodel, M. Abou-Ghanem, C. Gurganus, Y. Zhu, S. Tilmes, E. Ray, T. D. Thornberry, R.-S. Gao, E. J. Hintsa, F. Moore, G. Dutton, D. Nance, B. Hall, A. W. Rollins, E. M. Waxman, K. Zuraski, G. S. Diskin, Y. Choi, R. B. Pierce, B. Weinzierl, F. Kuderna, M. Dollner, E. Jensen, and C. A. Brock (2026). "An unrecognized mode of small particles in the lower stratosphere". *Science* 392.6796, eadw8939. DOI: 10.1126/science.adw8939.

Ma, C., H. Su, J. Lelieveld, W. Randel, P. Yu, M. O. Andreae, and Y. Cheng (2024). "Smoke-charged vortex doubles hemispheric aerosol in the middle stratosphere and buffers ozone depletion". *Science Advances* 10.28, eadn3657. DOI: 10.1126/sciadv.adn3657.

Pozzer, A., S. F. Reifenberg, V. Kumar, B. Franco, M. Kohl, D. Taraborrelli, S. Gromov, S. Ehrhart, P. Jöckel, R. Sander, V. Fall, S. Rosanka, V. Karydis, D. Akritidis, T. Emmerichs, M. Crippa, D. Guizzardi, J. W. Kaiser, L. Clarisse, A. Kiendler-Scharr, H. Tost, and A. Tsimpidi (2022). "Simulation of organics in the atmosphere: evaluation of EMACv2.54 with the Mainz Organic Mechanism (MOM) coupled to the ORACLE (v1.0) submodel". *Geoscientific Model Development* 15.6, pp. 2673–2710. DOI: 10.5194/gmd-15-2673-2022.

Pringle, K. J., H. Tost, S. Metzger, B. Steil, D. Giannadaki, A. Nenes, C. Fountoukis, P. Stier, E. Vignati, and J. Lelieveld (2010). "Description and evaluation of GMXe: a new aerosol submodel for global simulations (v1)". *Geosci. Model Dev.* 3.2, pp. 391–412. DOI: 10.5194/gmd-3-391-2010.

Randles, C. A., A. M. da Silva, V. Buchard, P. R. Colarco, A. Darmenov, R. Govindaraju, A. Smirnov, B. Holben, R. Ferrare, J. Hair, Y. Shinozuka, and C. J. Flynn (2017). "The MERRA-2 Aerosol Reanalysis, 1980 Onward. Part I: System Description and Data Assimilation Evaluation". *Journal of Climate* 30.17, pp. 6823–6850. DOI: 10.1175/JCLI-D-16-0609.1.

Su, B., T. Wang, G. Zhang, Y. Liang, C. Lv, Y. Hu, L. Li, Z. Zhou, X. Wang, and X. Bi (2022). "A review of atmospheric aging of sea spray aerosols: Potential factors affecting chloride depletion". *Atmospheric Environment* 290, p. 119365. ISSN: 1352-2310. DOI: j.atmosenv.2022.119365.